International Journal of Computer Science and Applications,

Vol. 12, No. 1, pp. 66 – 79, 2015

MODELING AND KINEMATICS STUDY OF HAND

Youwei Dong, Hieu N. Phan and Ahmed Rahmani

LAGIS UMR 8219 CNRS,
Ecole Centrale Lille,
59651 Villeneuve d'Ascq,
France

A control model of a designed mechanical model of the hand using Screw theory is presented. Forward and inverse kinematics of a finger, which is an open-chain manipulator with four degrees of freedom (DoF), is discussed. Forward kinematics are solved using the transformations in form of exponential of twist between the adjacent link frames to obtain the configuration of the fingertip frame T relative to the base frame S. For inverse kinematics, an algorithm is proposed to get the angle of rotation of the articulation, which is close to the palm, and Paden-Kahan sub problems are used to obtain the angles of rotation of the other articulations. The models of five fingers are integrated into a complete hand and the co-simulation results using Adams and Matlab confirm the feasibility and efficiency.

Keywords: hand; finger; modeling; forward kinematics; inverse kinematics; co-simulation.

Nomenclature

ω	axis of rotation, $\subset R^{3\times 1}$
$\hat{\omega}$	skew-symmetric matrix, $\in R^{3\times 3}$
θ	angle of rotation about the axis ω, rad
$e^{\hat{\omega}\theta}$	rotation matrix in R^3, $\in R^{3\times 3}$
$SO(3)$	$\{R \in R^{3\times 3}: RR^T = I, detR = 1\}$
$so(3)$	$\{S \in R^{3\times 3}: S^T = -S\}$
$\hat{\xi}$	twist, $\in R^{4\times 4}$
ξ	twist coordinates of $\hat{\xi}$, $\in R^{6\times 1}$
v	for rotation: $= -\omega \times q$; for translation: vector of velocity. $\subset R^{3\times 1}$
$e^{\hat{\xi}\theta}$	matrix of rigid motion, $\in R^{4\times 4}$
$SE(3)$	$\{(p, R): p \in R^3, R \in SO(3)\}$
$se(3)$	$\{(v, \hat{\omega}): v \in R^3, \hat{\omega} \in so(3)\}$

1. Introduction

The dexterous hand (DH) project is part of a mobile personal assistant robot, an intelligent system project involving artificial intelligence control techniques. The DH mainly consists of parts of the hand and corresponding movement mechanism to achieve delicate and complex operations. The hand, which is used to hold the elements, has a variety of structural forms depending on the form of the seized object, its size and weight, the material and the operational requirements. The movement mechanism is used to support the hand and achieve various rotations or oscillations, movements or a composite movement to achieve a certain operation to change the position and orientation of an object. The DoF is a key parameter in the design of the robot. With more degrees of freedom the hand is more flexible, but the structure is more complex. The purpose of the DH is to overcome the current operation limitations of a general robot and to expand the high-performance robot range of applications; for example, the robot could achieve delicate and complex operations and is capable of identifying the seized object.

In recent years increasing attention has been given to the modeling, control and simulation of the human hand, because of its crucial role in the design of humanoid robot and multi-fingered dexterous robot hand. Many universities and institutes have created different kinds of DH, for example, UTAH/MIT, PUMA/RAL and Stanford/JPL hands. A large number of papers in this domain have also been published. Liu et al. [Liu H. *et al.* (2008)] introduced in details a dexterous humanoid five-fingered robotic hand system. The kinematics complexity of the human hand and its complex structure with more than twenty DoFs make accurate modeling challenging, furthermore the stability and operation precision present very difficult modeling problems. Therefore simplified models have been developed to make kinematics and dynamics analyses easier. Hashimoto et al. [Hiroshi H. *et al*. (2011)] considered the DoF in the modeling of hand and developed a hand model, which is used for design tool of the industrial production. [Ramasamy S. and Arshad M.R. (2000)] simulated a robotic hand that emulates the shape and performance of a human hand; the simulation of result comes with analyses of the kinematics and dynamic properties. The developments of mathematics provide numerous methods to model the hand and solve the kinematics. Liu, Zhu and Wang [Songguo L. *et al.* (2008)] proposed a real-time and high-accuracy performances optimized algorithm to solve the procedure complexity and extraneous roots problem of the existing real time algorithms for general 6R robots inverse kinematics. Like in many other papers, the Denavit- Hartenberg parameters are used. Screw theory is introduced in the work of Murray, Li and Sastry [Richard M. M. *et al.* (1994)]. This tool allows a global description of rigid body motion without suffering from the singularities due to the use of local coordinates. It also provides a geometric description of rigid motion, which greatly simplifies the analysis of mechanisms.

This paper is organized as follows: firstly the mechanical designed hand [Qian Y. (2013)] (using CATIA Software) is presented; secondly, the forward and inverse kinematics are discussed, and useful results are given; then a co-simulation using Adams and Matlab is proposed to confirm the calculation results; the final section is the paper conclusions.

2. Design of Hand

For the design of a humanoid manipulator, the transmission should be stable and reliable, and the structure should be simple to guarantee the facility of the maintenance. To imitate human hand, five fingers are given, and there is a revolute joint for each finger articulation. The fingers except the thumb have almost identical structure, whereas the thumb is most flexible. We allocate 4 DoFs to each finger, while in order to simplify the model, none DoF is given to the palm. Thus there are totally 20 DoFs for such a hand. The palm and all the fingers are hollow to reserve space for sensors and motors; each individual joint is driven by a steering gear both to reduce the accumulated error and to enhance the stability of grasping.

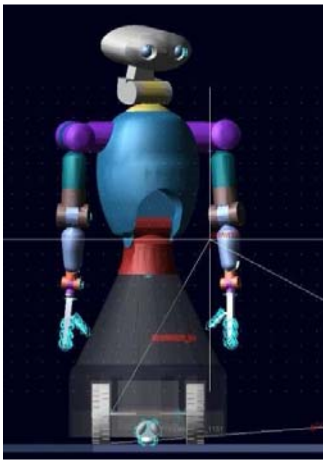

Fig. 1. Virtual model of mobile personal assistant robot

The structure of the whole hand is created in Catia V5, as shown in Fig. 2 and Fig. 3. The articulations of each finger are numbered by 1, 2, 3 and 4. And the corresponding lengths are respectively: 21.00mm, 28.53mm, 27.16mm and 18.50mm.

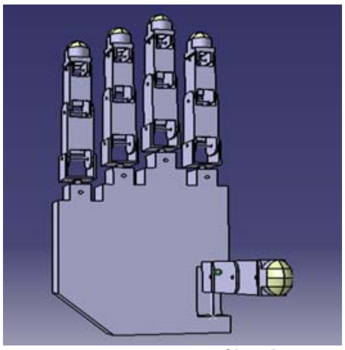

Fig. 2. Structure of hand

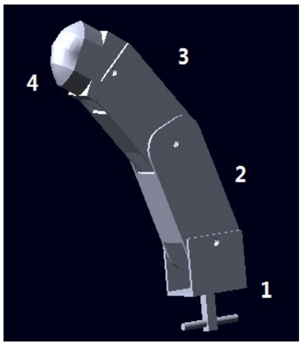

Fig. 3. Structure of finger

3. Kinematics of One Finger

3.1. *Coordinate frames*

The configuration of a rigid body is represented by attaching a Cartesian coordinate frame to a certain point on the rigid body and keeping track of the motion of this body coordinate frame relative to a fixed frame. We could retrieve the motion of the individual particles of each body from the motion of the body frame and the motion of the point of attachment of the frame to the body. In this paper, all coordinate frames are required to be right-handed: three orthonormal vectors $x, y, z \in R^3$, which define a coordinate frame, should satisfy $z = x \times y$.

To define the task of the whole hand, it is necessary to define the configuration of each finger; as a result, we will study the kinematics of a finger. The coordinate frames are created as shown in Fig. 4. We suppose that the frame [*S*, *XYZ*] is fixed. There is a coordinate frame attached on the point of each joint: [q_i, *XYZ*] (i=2,3,4), and a tool frame [*T*, *XYZ*] attached on the fingertip T. Because of the joint on the point S, the finger could rotate about the axis Y, and the other joints on the points q_i(i=2,3,4) result in the rotations about the axis X. Modeling in Maple, we could obtain the workspace of the finger, as shown in Fig. 4.

3.2. *Transformation matrix*

The elements of screw theory can be traced to the work of Chasles and Poinsot in the early 1800s. Chasles proved that every rigid body motion can be realized by a rotation about an axis combined with a translation parallel to that axis (Chasles' theorem). This motion is called screw motion, and the infinitesimal version of a screw motion is a twist [Richard M. M. *et al.* (1994)].

We use $g: R^3 \rightarrow R^3$ to represent a rigid body transformation, which satisfies the following properties:

(1) Length is preserved: $\|g(p) - g(q)\| = \|p - q\|$ for all points $p, q \in R^3$;

(2) The cross product is preserved for all vectors $v, w \in R^3$: $g_*(v \times w) = g_*(v) \times g_*(w)$.

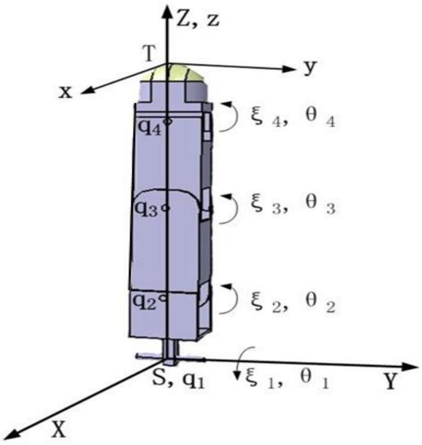

Fig. 4. Coordinate frames

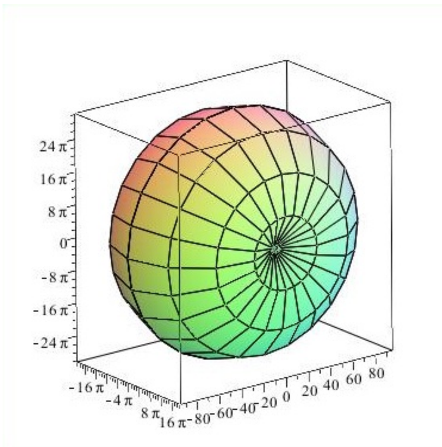

Fig. 5a. Workspace of finger for $\theta_1 \in [0, 2\pi]$ and for $\theta_1 \in [-10°, 10°]$

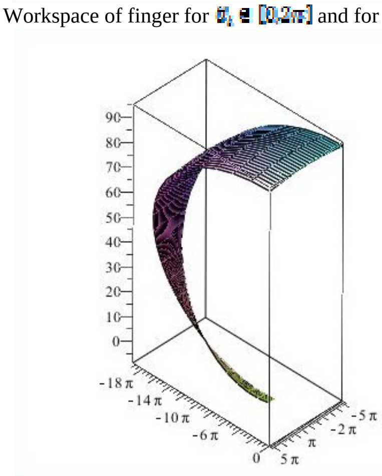

Fig. 5b. Workspace of finger for $\theta_1 \in [0, 5\pi]$ and for $\theta_{2,3,4} \in [0°, 88°]$

We note that the operator $\wedge$ is:

$$(a)^\wedge = \hat{a} = \begin{bmatrix} 0 & -a_3 & a_2 \\ a_3 & 0 & -a_1 \\ -a_2 & a_1 & 0 \end{bmatrix}.$$

Some notations are adopted for the homogeneous representation: we add 1 to the coordinates of a point to yield a vector in R^4 and 0 to the coordinates of a vector:

$$q = [q_1 \quad q_2 \quad q_3 \quad 1]^T, v = [v_1 \quad v_2 \quad v_3 \quad 0]^T.$$

By using the homogeneous representation, the transformation $g = (p, R)$ of the rigid motion in R^3, where $p \in R^{3\times1}$ is the translation of the rigid and $R \in R^{3\times3}$ is the rotation matrix, could be represented by a 4×4 matrix:

Case 1 ($\omega = 0$): If the rotation vector is null:

$$g = e^{\hat{\xi}\theta} = \begin{bmatrix} I & v\theta \\ 0 & 1 \end{bmatrix} \tag{1}$$

Case 2 ($\omega \neq 0$): this is the normal motion (there are both movement and rotation):

$$g = e^{\hat{\xi}\theta} = \begin{bmatrix} e^{\hat{\omega}\theta} & (I - e^{\hat{\omega}\theta})(\omega \times v) + \omega\omega^T v\theta \\ 0 & 1 \end{bmatrix} \tag{2}$$

where

$$e^{\hat{\omega}\theta} = I + \hat{\omega}sin\theta + \hat{\omega}^2(1 - cos\theta) \qquad \|\omega\| = 1 \tag{3}$$

Thus we could represent the transformation of a point (or a vector): $q_a = g_{ab}q_b$.

For the analysis of kinematics of a finger, which is an open-chain mechanism, we define $g_{l_{i-1}l_i}(\theta)$ as the transformation between the adjacent link frames, and then the overall kinematics of this system is given by

$$g_{st}(\theta) = g_{sl_1}(\theta_1)g_{l_1l_2}(\theta_2)\cdots g_{l_{n-1}l_n}(\theta_n)g_{l_nt} \tag{4}$$

3.3. *Forward kinematics*

The forward kinematics of a robot determines the configuration of the end-effector (the gripper of tool mounted on the end of the robot) given the relative configurations of each pair of adjacent links of the robot.

We let $g_{st}(0)$ represent the initial configuration of a rigid body relative to a frame A, then the final configuration is given by $g_{ab}(\theta) = e^{\hat{\xi}\theta}g_{st}(0)$.

With the exponential expression for the rigid motion, Eq. 4 becomes:

$$g_{st}(\theta) = e^{\hat{\xi}_1\theta_1}e^{\hat{\xi}_2\theta_2}\cdots e^{\hat{\xi}_n\theta_n}g_{st}(0) \tag{5}$$

According to the design of the hand, the lengths of each articulation are: l_1=21.00mm, l_2=28.53mm, l_3=27.16mm and l_4=18.50mm. In Fig. 4, we observe that the transformation between tool and base frame at $\theta = 0$ is given by:

$$g_{st}(0) = \begin{bmatrix} 1 & 0 & 0 & 0 \\ 0 & 1 & 0 & 0 \\ 0 & 0 & 1 & \sum_{i=1}^{4} l_i \\ 0 & 0 & 0 & 1 \end{bmatrix}.$$

To construct the twists for the revolute joints, note that $\omega_1 = [0 \quad 1 \quad 0]^T$, and $\omega_2 = \omega_3 = \omega_4 = [1 \quad 0 \quad 0]^T$.

And we choose the axis point of the joint: $q_1 = [0 \quad 0 \quad 0]^T$, $q_2 = [0 \quad 0 \quad l_1]^T$, $q_3 = [0 \quad 0 \quad l_1 + l_2]^T$ and $q_4 = [0 \quad 0 \quad l_1 + l_2 + l_3]^T$ which yields the corresponding vector and twist of the joint 1: $v_1 = -\omega_1 \times q_1 = [0 \quad 0 \quad 0]^T$, $\xi_1 = [v_1 \quad \omega_1]^T = [0 \quad 0 \quad 0 \quad 0 \quad 1 \quad 0]^T$.

According to Eq. 2, the individual exponential is given by

$$e^{\hat{\xi}_1 \theta_1} = \begin{bmatrix} cos\theta_1 & 0 & sin\theta_1 & 0 \\ 0 & 1 & 0 & 0 \\ -sin\theta_1 & 0 & cos\theta_1 & 0 \\ 0 & 0 & 0 & 1 \end{bmatrix}.$$

Using the same method, we can solve the transformations of the other joints. Executing the symbolic computation in Maple, we get the full forward kinematics:

$$g_{st}(\theta) = e^{\hat{\xi}_1 \theta_1} e^{\hat{\xi}_2 \theta_2} e^{\hat{\xi}_3 \theta_3} e^{\hat{\xi}_4 \theta_4} g_{st}(0) = \begin{bmatrix} R(\theta) & p(\theta) \\ 0 & 1 \end{bmatrix}$$

Where

$$R(\theta) = \begin{bmatrix} r_{11} & r_{12} & r_{13} \\ r_{21} & r_{22} & r_{23} \\ r_{31} & r_{32} & r_{33} \end{bmatrix}, \quad p(\theta) = \begin{bmatrix} p_1 \\ p_2 \\ p_3 \end{bmatrix},$$

and using the notation $c_i = cos\theta_i$, $s_i = sin\theta_i$,

$r_{11} = c_1$, $r_{21} = 0$, $r_{31} = -s_1$,

$r_{12} = (s_1 s_2 c_3 + s_1 c_2 s_3)c_4 + (-s_1 s_2 s_3 + s_1 c_2 c_3)s_4$,

$r_{13} = -(s_1 s_2 c_3 + s_1 c_2 s_3)s_4 + (-s_1 s_2 s_3 + s_1 c_2 c_3)c_4$,

$r_{22} = (c_2 c_3 - s_2 s_3)c_4 + (-c_2 s_3 - s_2 c_3)s_4$,

$r_{23} = (s_2 s_3 - c_2 c_3)s_4 - (c_2 s_3 + s_2 c_3)c_4$,

$r_{32} = (c_1 s_2 c_3 + c_1 c_2 s_3)c_4 + (-c_1 s_2 s_3 + c_1 c_2 c_3)s_4$,

$r_{33} = -(c_1 s_2 c_3 + c_1 c_2 s_3)s_4 + (-c_1 s_2 s_3 + c_1 c_2 c_3)c_4$,

$p_1 = (-(s_1 s_2 c_3 + s_1 c_2 s_3)s_4 + (-s_1 s_2 s_3 + s_1 c_2 c_3)c_4)(l_1 + l_2 + l_3 + l_4)$
$+((s_1 s_2 c_3 + s_1 c_2 s_3)s_4 + (-s_1 s_2 s_3 + s_1 c_2 c_3)(1 - c_4))(l_1 + l_2 + l_3)$
$+(s_1 s_2 s_3 + s_1 c_2 (1 - c_3))(l_1 + l_2) + s_1 (1 - c_2) l_1$,

$p_2 = (-(c_2 c_3 - s_2 s_3)s_4 + (-c_2 s_3 - s_2 c_3)c_4)(l_1 + l_2 + l_3 + l_4)$
$+((c_2 c_3 - s_2 s_3)s_4 + (-c_2 s_3 - s_2 c_3)(1 - c_4))(l_1 + l_2 + l_3)$
$+(c_2 s_3 - s_2 (1 - c_3))(l_1 + l_2) + s_2 l_1$,

$p_3 = (-(c_1 s_2 c_3 + c_1 c_2 s_3)s_4 + (-c_1 s_2 s_3 + c_1 c_2 c_3)c_4)(l_1 + l_2 + l_3 + l_4)$
$+((c_1 s_2 c_3 + c_1 c_2 s_3)s_4 + (-c_1 s_2 s_3 + c_1 c_2 c_3)(1 - c_4))(l_1 + l_2 + l_3)$

$+(c_1 s_2 s_3 + c_1 c_2 (1 - c_3))(l_1 + l_2) + c_1(1 - c_2) l_1$

If we let for example $\theta_1 = \pi/4$, $\theta_2 = \theta_3 = \theta_4 = \pi/6$, we have the numeric matrix

$$g_{st}(\theta) = \begin{bmatrix} 0.7071 & 0.7071 & 0.0000 & 41.9227 \\ 0.0000 & 0.0000 & -1.0000 & -56.2862 \\ -0.7071 & 0.7071 & 0.0000 & 41.9227 \\ 0 & 0 & 0 & 1 \end{bmatrix}$$

The 3×3 matrix $\begin{bmatrix} 0.7071 & 0.7071 & 0.0000 \\ 0.0000 & 0.0000 & -1.0000 \\ -0.7071 & 0.7071 & 0.0000 \end{bmatrix}$ represents the coordinates of each axe of frame T relative to frame S which is the fixed frame attached on the point S, and $[41.9227 \quad -56.2862 \quad 41.9227]^T$ is the position of the fingertip in frame S.

3.4. *Inverse kinematics*

Given a desired configuration for the tool frame, the inverse kinematics problem is to find joint angles, which achieve that configuration. That is, given a forward kinematics map $g_{st}: Q \to SE(3)$ and a desired configuration $g_d \in SE(3)$, we would like to solve the equation $g_{st}(\theta) = g_d$ for some $\theta \in Q$.

If a desired configuration for the tool frame T is given, the problem is to find joint angles, which achieve that configuration. That is to solve the equation $g_{st}(\theta) = g_d$ where g_{st} is a forward kinematics map. According to the forward kinematics of the finger, we get the equation

$$e^{\hat{\xi}_1\theta_1} e^{\hat{\xi}_2\theta_2} e^{\hat{\xi}_3\theta_3} e^{\hat{\xi}_4\theta_4} = g_d g_{st}^{-1}(0) \tag{6}$$

We observe in Fig. 6 that the first angle of rotation θ_1, which is formed by Y axis and the projection of the finger on X-Z plane, depends on the position and orientation of the fingertip. As a result, an algorithm is proposed to generate this angle, and we limit it within $(-\pi/2, \pi/2)$.

Algorithm 1: Computing θ_1

Input: a desired configuration $g = \begin{bmatrix} R & p \\ 0 & 1 \end{bmatrix}$ where R is a 3×3 matrix and p is a three-dimensional vector.

if $R(1,3) = 0$ then

  if $p(1) = 0$ then

    $\theta_1 \leftarrow 0$

  else

    $\theta_1 \leftarrow \left(\frac{\pi}{2} - \left|\arctan\left(\frac{p(3)}{p(1)}\right)\right|\right) \cdot sign(p(1))$

  end if

else

$$\alpha \leftarrow \arctan\left(\frac{n(2,3)}{n(1,3)}\right),$$

$$\theta_1 \leftarrow \left(\frac{\pi}{2} - |\alpha|\right) \cdot sign(\alpha)$$

end if

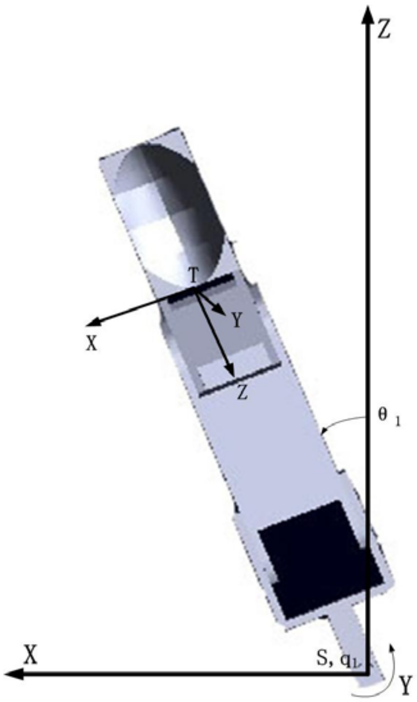

Fig. 6. Configuration of finger

This algorithm gives the value of θ_1, and Eq. 6 becomes

$$e^{\hat{\xi}_2\theta_2} e^{\hat{\xi}_3\theta_3} e^{\hat{\xi}_4\theta_4} = \left(e^{\hat{\xi}_1\theta_1}\right)^{-1} g_d\, g_{st}^{-1}(0) =: u_0 \tag{7}$$

By applying the Paden-Kahan subproblem [Richard M. M. *et al.* (1994), Paden B. (1986)] 1 and 3, the other angles could be solved. We take the points defined in Fig. 3, and use the operation $e^{\hat{\xi}\theta} p = p$ if p is on the axis of a revolute twist ξ. Applying both sides of Eq. 7 to the point q_4 on the axis of ξ_4 yields:

$$e^{\hat{\xi}_2\theta_2} e^{\hat{\xi}_3\theta_3} q_4 = u_0 q_4 =: u_1 \tag{8}$$

We subtract the point q_2 on both sides of this equation and take the norm of the result, then we have:

$$\left\| e^{\hat{\xi}_2\theta_2} e^{\hat{\xi}_3\theta_3} q_4 - q_2 \right\| = \left\| u_1 - q_2 \right\| \Rightarrow \left\| e^{\hat{\xi}_3\theta_3} q_4 - q_2 \right\| = \left\| u_1 - q_2 \right\|.$$

This is just the Paden-Kahan subproblem 3; using the formula and the limitation of angles, we could obtain θ_3:

$$\theta_3 = \theta_0 - arccos\left(\frac{\|u'\|^2 + \|v'\|^2 - \delta'^2}{2\|u'\|^2\|v'\|^2}\right)$$

where $\theta_0 = atan2(\omega_3{}^T(u' \times v'), u'^T v')$, and u', v', δ' are the projections of q_4, q_2 and $u_1 - q_2$ onto the plane perpendicular to the axis of revolution ω_3.

Now Eq. 8 becomes the Paden-Kahan subproblem 1, and we could have θ_2: $\theta_2 = atan2(\omega_2{}^T(u' \times v'), u'^T v')$ where u', v' are the projections of $e^{\hat{\xi}_3\theta_3} q_4$ and u_1 onto the plane perpendicular to the axis of revolution ω_2.

Then we have only θ_4 to solve. Eq. 7 becomes:

$$e^{\hat{\xi}_4\theta_4} = \left(e^{\hat{\xi}_3\theta_3}\right)^{-1}\left(e^{\hat{\xi}_2\theta_2}\right)^{-1}\left(e^{\hat{\xi}_1\theta_1}\right)^{-1} g_d g_{st}^{-1}(0) =: u_2$$

We multiply the fingertip point T to both sides of this equation, and we obtain again a Paden-Kahan subproblem 1. So we have θ_4: $\theta_4 = atan2\left(\omega_4{}^T(u' \times v'), u'^T v'\right)$ where u', v' are the projections of T and $u_2 T$ onto the plane perpendicular to the axis of revolution ω_4.

Maple Software is used to avoid the cumulative error of floating-point computation, and then take the matrix of the example in last section:

$$g_{st}(\theta) = \begin{bmatrix} 0.7071 & 0.7071 & 0.0000 & 41.9227 \\ 0.0000 & 0.0000 & -1.0000 & -56.2862 \\ -0.7071 & 0.7071 & 0.0000 & 41.9227 \\ 0 & 0 & 0 & 1 \end{bmatrix},$$

we then find all the angles:

$$\theta_1 = \pi/4,\ \theta_2 = \theta_3 = \theta_4 = \pi/6.$$

3.5. *Co-simulation of one finger*

We can carry out a co-simulation of the finger with Adams and Matlab after importing the model designed in Catia into Adams. The model of simulation in Matlab is shown in Fig. 7.

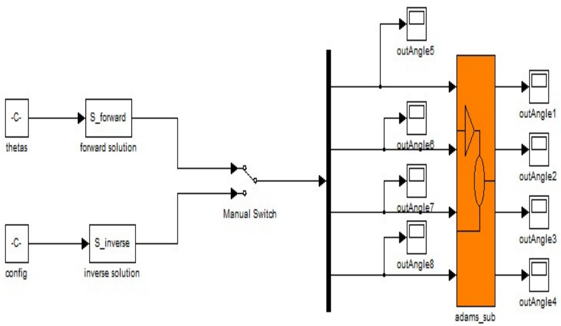

Fig. 7. Model of co-simulation

The two branches are for solving respectively the forward and inverse kinematics, and the processes of the inputs are programmed in two S-function: for the forward kinematics, the input is a vector of the four angles of rotation; for inverse kinematics, the input is a desired configuration which is a 4×4 matrix. The duration of simulation is 5 seconds. After executing this model, the animation and graphical results (Fig. 8) confirm that our model is correct and has a good precision.

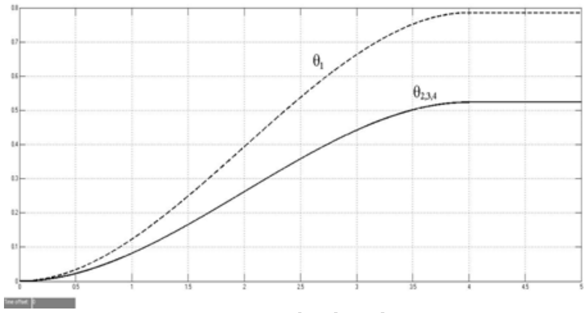

Fig. 8. Graphical results

3.6. *Integration and co-simulation*

Now we can do the same thing for the other 4 fingers. The fixed frame should be attached to the palm, and a new transformation matrix should be multiplied to Eq. 5 for each finger:

$$g_{st}(\theta) = Z e^{\hat{\xi}_1\theta_1} e^{\hat{\xi}_2\theta_2} \cdots e^{\hat{\xi}_n\theta_n} g_{st}(0) \tag{9}$$

where Z is the transformation matrix defining the location of the finger (frame $S_i, i = 1, \cdots, 5$) relative to the world frame shown in Fig. 9.

According to the design of the hand in Catia, we can determine the five Z for each finger:

$$Z_1 = \begin{bmatrix} 1 & 0 & 0 & 0 \\ 0 & 0 & 1 & 0 \\ 0 & -1 & 0 & 0 \\ 0 & 0 & 0 & 1 \end{bmatrix}, \quad Z_2 = \begin{bmatrix} 1 & 0 & 0 & 2 \\ 0 & 1 & 0 & -7 \\ 0 & 0 & 1 & 70 \\ 0 & 0 & 0 & 1 \end{bmatrix}, \quad Z_3 = \begin{bmatrix} 1 & 0 & 0 & 22 \\ 0 & 1 & 0 & -7 \\ 0 & 0 & 1 & 80 \\ 0 & 0 & 0 & 1 \end{bmatrix},$$

$$Z_4 = \begin{bmatrix} 1 & 0 & 0 & 42 \\ 0 & 1 & 0 & -7 \\ 0 & 0 & 1 & 70 \\ 0 & 0 & 0 & 1 \end{bmatrix}, \quad Z_5 = \begin{bmatrix} 1 & 0 & 0 & 62 \\ 0 & 1 & 0 & -7 \\ 0 & 0 & 1 & 60 \\ 0 & 0 & 0 & 1 \end{bmatrix}.$$

To carry out a co-simulation, we define a simple task which is to support a plane Y=60mm. And we determine the five configurations of the fingers as the input of the simulation:

$$g_2 = \begin{bmatrix} \frac{2}{\sqrt{5}} & \frac{1}{\sqrt{5}} & 0 & -13 \\ 0 & 0 & 1 & 60 \\ \frac{1}{\sqrt{5}} & -\frac{2}{\sqrt{5}} & 0 & 100 \\ 0 & 0 & 0 & 1 \end{bmatrix}, \quad g_1 = \begin{bmatrix} 1 & 0 & 0 & 0 \\ 0 & 0 & 1 & 60 \\ 0 & -1 & 0 & -50 \\ 0 & 0 & 0 & 1 \end{bmatrix}, \quad g_3 = \begin{bmatrix} 1 & 0 & 0 & 22 \\ 0 & 0 & 1 & 60 \\ 0 & -1 & 0 & 120 \\ 0 & 0 & 0 & 1 \end{bmatrix},$$

$$g_4 = \begin{bmatrix} \frac{2}{\sqrt{5}} & -\frac{1}{\sqrt{5}} & 0 & 57 \\ 0 & 0 & 1 & 60 \\ -\frac{1}{\sqrt{5}} & -\frac{2}{\sqrt{5}} & 0 & 100 \\ 0 & 0 & 0 & 1 \end{bmatrix}, \quad g_5 = \begin{bmatrix} \frac{1}{\sqrt{5}} & -\frac{2}{\sqrt{5}} & 0 & 92 \\ 0 & 0 & 1 & 60 \\ -\frac{2}{\sqrt{5}} & -\frac{1}{\sqrt{5}} & 0 & 75 \\ 0 & 0 & 0 & 1 \end{bmatrix}.$$

Knowing Z and *g* and using the inverse kinematics model of one finger, all the angles of each finger could be solved. So there should be a 20-dimensional vector outputted for the part of Adams. Then after importing the model designed in Catia into Adams, we can carry out the co-simulation of the whole hand with Adams and Matlab. The model of simulation in Matlab is shown in Fig. 10.

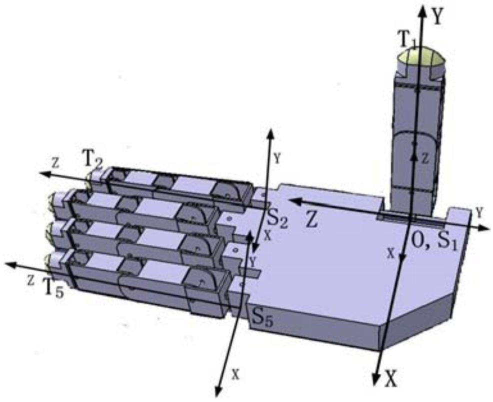

Fig. 9. Frames of the hand

The input is a 1×80 vector, which defines the configurations of the five fingers relative to the world frame; for each finger, 16 parameters form a 4×4 transformation matrix. The process of treating the inputs is programmed in an S-function file, which exports a 1×20 vector as the angles of rotation of the 20 articulations. The duration of simulation is 5 seconds. After executing this model, the animation and graphical result shown in Fig. 11 (the plane is not displayed) and Fig. 12 confirm that our model is correct. The results demonstrate that this model could achieve any task in the workspace of the hand.

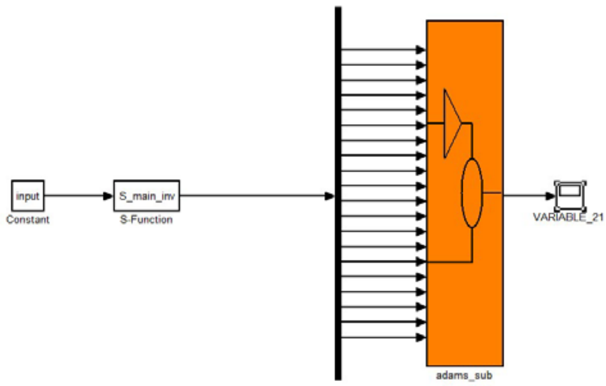

Fig. 10. Model of co-simulation

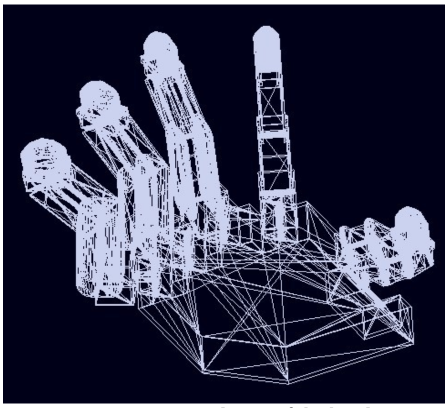

Fig. 11. Simulation of the hand

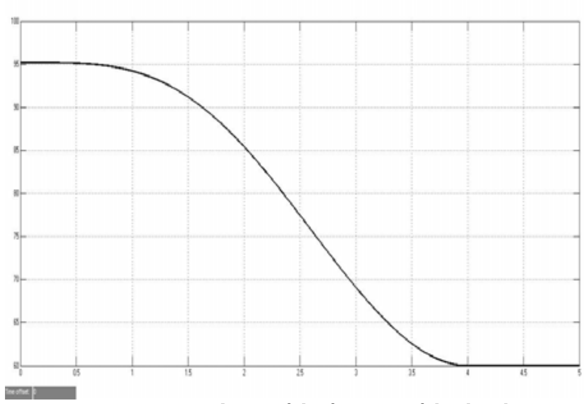

Fig. 12. Y coordinate of the fingertip of the thumb

4. Conclusion

A new 3D model of hand is created in Catia and the finger forward and inverse kinematics are analyzed by using screw theory (each finger has 4 DoFs). Having the reachable workspace of a finger calculated, using Matlab and Adams the co-simulation of one finger and of the hand is executed to confirm the results of calculation: the hand model could realize any position and configuration in its workspace.

The 4×4 transformation matrix containing the information of the four joints for each finger is obtained without extraneous root by using symbolic computation. Thus avoiding the cumulative error of floating-point computation and improve the stability and precision of the model.

There is one major problem which needs to be addressed: the dynamics, e.g.: force and velocity must be considered. As future research, we are aiming to build a dynamic model of the human hand.

References

Hiroshi H., Akinori S., Sho Y., Yasuhiro O., Chiharu I. (2011) : *A Study on Degree of Freedom in Hand Modeling*. SICE Annual Conference, Waseda University, Tokyo, Japan. Sep.13-18,2011, p.2492.

Liu H., Wu K., Meusel P., Hirzinger G., Jin M.H., Liu Y.W., Fan S.W., Lan T., Chen Z.P. (2008): *A Dexterous Humanoid Five-fingered Robotic Hand*. 17^{th} IEEE International Symposium on Robot and Human Interactive Communication, Technische Universitat Munchen, Munich, Germany, p.371.

Paden B. (1986): *Kinematics and Control Robot Manipulators*. PhD thesis, Department of Electrical Engineering and Computer Sciences, University of California, Berkeley.

Qian Y. (2013): *Design and Control of a Personal Assistant Robot*. PhD thesis, Laboratoire d'Automatique Génie Informatique et Signal, Ecole Centrale de Lille.

Ramasamy S. and Arshad M.R. (2000): *Robotic Hand Simulation with Kinematics and Dynamic analysis*. Tencon. Proceedings. Vol.3, p.178.

Richard M. M., Zexiang L. and Shankar S.S. (1994): *A Mathematical Introduction to Robotic Manipulation*.

Songguo L., Shiqiang Z., Xuanyin W. (2008): *Real-time and High-accurate Inverse Kinematics Algorithm for General 6R Robots Based on Matrix Decomposition*. Chinese Journal of Mechanical Engineering, Vol.44, No.11, p.304.